Summer Internship Report

PZT based high voltage generator for chip-scale gas-sensor

Manikandan Srinivasan

SonicMEMS lab,
School of Electrical and Computer Engineering, Cornell University

July 17, 2014

Outline

Principles of operation for gas sensing and limitations

- Recently, gas sensing, as a typical application in intelligent systems, is receiving increasing attention in both industry and academia.
- Detection of trace concentration of gases is a critical component in many industrial and medical applications.
- Conventional methods of gas sensing are limited by:
  Sensitivity to only a single specific gas
  Large response times in detection
  Not suitable for miniaturization
  Large input voltage and power for operation
  Higher cost

Outline

Ion-mobility spectrometer

- Low-voltage ion-mobility spectrometer array[1] developed in the lab relies on the charges and masses of molecules to separate and detect multiple species of gas-phase ionized molecules in a buffer gas.

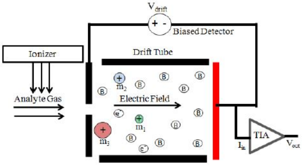

Figure: Ion-mass spectrometer

- The figure above describes the working principle of the ion-mobility spectrometer- The gas molecules are ionized at the inlet and they are drifted to different distances depending on the charge and mass of the ions.

Ion-mobility spectrometer array developed in lab

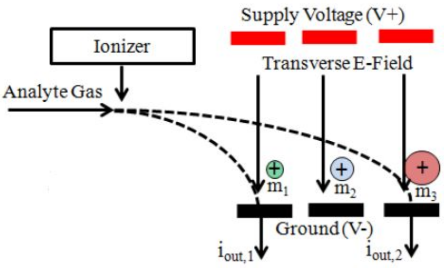

Figure: Ion-mass spectrometer array

- For example, presence of 3 electrodes at appropriate locations enables us to detect 3 different gas molecules in a mixture of gases.
- If needed, more electrode pairs can be used.

- Higher bias voltage of the electrode plates- making drift tube longer- enables us to get a better temporal and spatial resolution of the gas molecules.
  We know that,
  $$v_{drift} = \mu E$$
  where μ is the mobility of the ions in the buffer gas given by the Mason-Schamp equation[2]
  $$\mu = \frac{3}{16}\sqrt{\frac{2\pi}{m_{eff}kT}}\frac{q}{n\sigma}$$
  where m_{eff} is the reduced mass of the ion in the buffer gas, q is ion charge, σ is the collision cross section of the ion and n is ambient air concentration.
- The ion with the largest charge to mass ratio is detected at the farthest electrode.

Outline

The need for air-ionizer

- Ion-mobility spectrometer array requires ionized mixture of gas molecules for it to function.
- In order to develop a chip scale gas sensor, it is necessary to develop a miniaturized lower voltage ionizer.
- A simple and an effective way- Apply large enough electric field to cause a dielectric breakdown of the gaseous mixture.

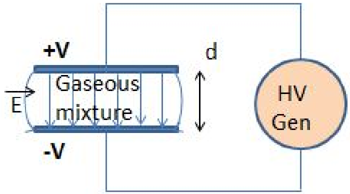

Figure: Capacitor-dielectric arrangement

A small calculation

Let us consider ambient air to be our test "gaseous mixture".
The dielectric strength of ambient air[3] is $3.0 \, \mathrm{x} \, 10^6 \, \mathrm{V/m}$.

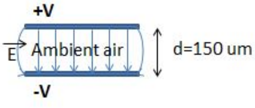

Figure: Electrodes separated by a distance- Parallel plate capacitor

Calculation

$$V_{br} = \frac{E_{br} d}{2} = 225 \ V$$

Outline

Micro-machining PZT bimorph

- PZT bimorph cantilever beams were fabricated using a commercial laser tool- *LPKF Protolaser U*
- Process flow that had been developed developed[3] was used to to create structures and electrode patterns on bulk PZT-4 that is polled in its thickness direction.

Process flow

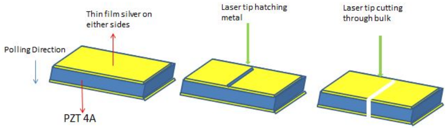

Figure: Describes the process flow for micro-machining PZT

Outline

In-plane actuation of PZT bimorph cantilever beam

- PZT cantilever beams are micro-machined with a definite electrode patterning for in-plane actuation[3].

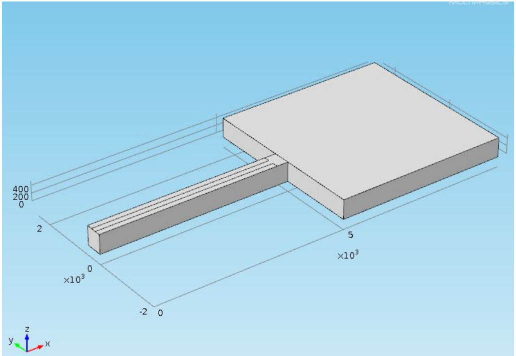

Figure: Schematic of the cantilever beam. The silver electrodes (the two rectangular blocks) are patterned on the top side and the bottom surface has thin-film silver.

Actuation mechanism of the beam

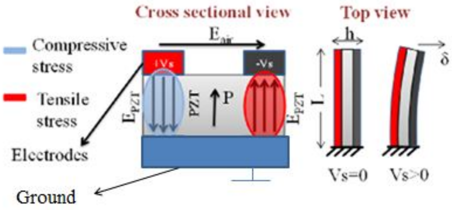

Figure: Simple illustration of the actuation-mechanism

- The bottom surface of the device is grounded.
- Assuming that the beam is actuated with DC, a +ve voltage is applied at one electrode and -ve is applied at another.
- Electric field is generated as show in the illustration above.

Applying the mathematical model of inverse-piezoelectricity,

$$s = \begin{bmatrix} 0 & 0 & d_{31} \\ 0 & 0 & d_{32} \\ 0 & 0 & d_{33} \\ 0 & d_{24} & 0 \\ d_{15} & 0 & 0 \end{bmatrix} \times [E_1 \quad E_2 \quad E_3]^T$$

where s is the strain vector and E_1,E_2 and E_3 represent fields in x,y and z directions of the cantilever beam respectively.

- For in-plane mode, d_{31} component contributes resulting in strain along the longitudinal direction.
- Due to the different directions of electric fields along thickness as we move along the y direction, some parts are under tension (elongation) and other parts are in compressive stress (compression) resulting in bending.

Outline

High voltage generation idea

- Instead of applying DC voltages to electrodes, AC voltages when applied to electrodes may result in in-plane oscillations.
- The cantilever is driven by out-of-phase sinusoids at resonant frequency.
- At resonance the amplitude of oscillations can be very high.
- The stress (hence the strain) at the anchor of any cantilever beam is the maximum generated in the beam.
- If there is a way to harness the potential due to direct piezoelectric effect, the high strain at the anchors may perhaps give high voltages.

Outline

Finite element analysis

- Though several device dimensions were simulated and then fabricated, the following device specifications seemed to give the best performance (both in simulation and in experiment).

Device specifications

The cantilever beam has the following dimensions

- length 5000 μm
- width 900 μm
- height 500 μm
  The width of the electrode is 150 microns each on the top plate (+5 and -5V_p AC signal is applied) and bottom surface is grounded completely.
  To simulate damping, material isotropic loss factor was set to 1/1000

Finite element analysis

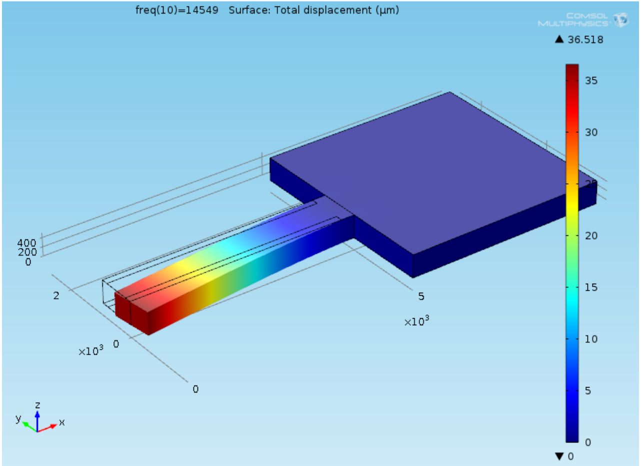

Figure: Displacement profile at resonant frequency of 14549 Hz

Finite element analysis

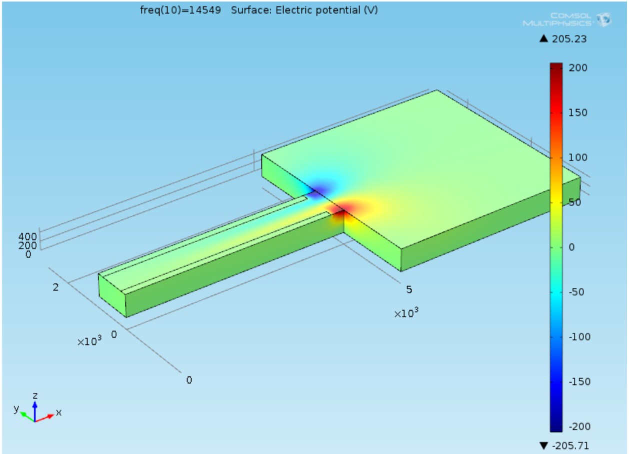

Figure: Surface potential profile at resonant frequency of 14549 Hz

More designs

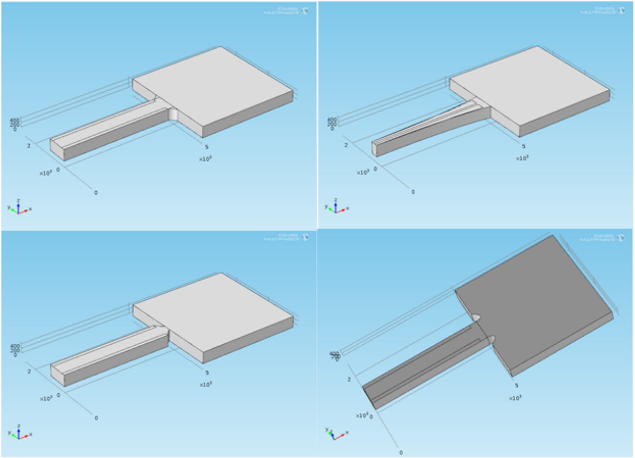

Figure: Though different designs were simulated (and subsequently fabricated), there was a very little difference in performance

Outline

Output stage differential Op-Amp

Since the looking in-capacitance and leakage current due to loading effect plays a considerable role in deteriorating, differential op-amp at the output stage is needed for testing purposes.

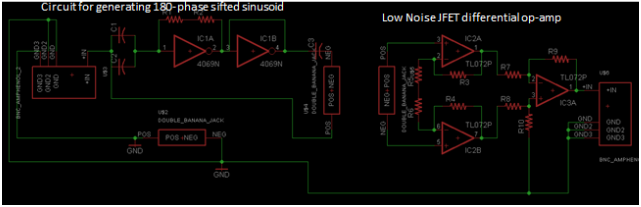

The differential opamp has a self-gain of 1.9.Thus all our measurements are scaled down by this factor to compensate.

Testing and Results

- Tried various different configurations for testing HV.
- Reported results are for the 900 um wide 5 mm long beam with the 3 sense electrode configurations as shown in the following figure.

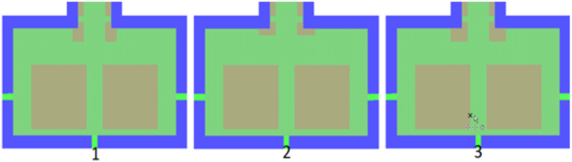

Figure: Different sense electrode configurations - 1 has a 150x150 square cut out from 450x300 rectangle, 2 has a 150x300 cut in a 450x300 horizontal rectangle and 3 has 150x300 cut in a 450x450 square all units in μm^2

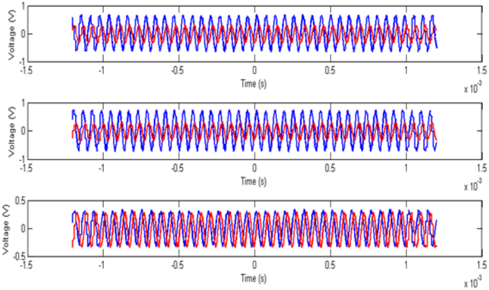

Figure: Outputs for sense electrode configurations 1, 2 and 3. Red curves are inputs and blue are outputs

- The outputs in the figure show gains of *0.95*, *1.1* and *0.48* respectively (normalising for the opamp-gain).
- As expected, configuration 2 produces best performance due to low capacitance and large contact area with the edge of anchor.

- The results are not according to what we expected from simulation.

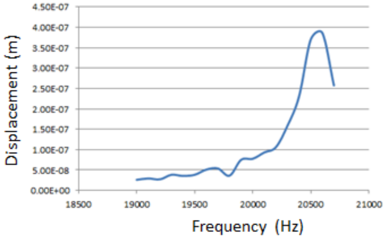

Figure: In-plane displacement vs frequency of the input voltage

- One possible reason for not getting high enough voltage could be because of small in-plane tip displacement (370 nm at resonance when tested as compared to 36.51 μm in simulation).
- Explanation for this difference is still unknown (reasons could be quality factor, damping, fabrication technique or improper actuation scheme).

Outline

Macro-scale PZT transformer

- The idea of PZT transformer was first implemented by Rosen in 1956[4]

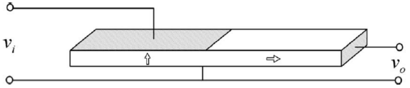

Figure: Structure of Rosen type piezoelectric transformer

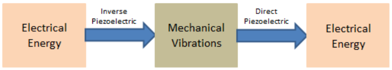

Figure: Working principle

- The voltage gain at resonance is proportional to the aspect ratio of the transformer.

Limitations of PZT type transformer

- Unlike electromechanical transformers, the efficiency and voltage conversion ratio depends on the frequency of the input voltage (since the coupling is mechanical and mechanical systems are frequency dependent)
- Efficiency and voltage conversion ratio are maximum at resonant frequency. However, the value of resonant frequency changes significantly with loading.
- Rosen type transformers require polling in two directions and electrode patterning on three surfaces making it difficult for batch fabrication.
- Electromechanical coupling coefficient is usually low in Rosen based transformers and hence the efficiency
- Research[5][6] is now done on making disk-based resonators which involve only a single polling process.

Outline

Construction of disk-PZT transformers

- The following figure shows PT with external radius R and thickness h ($h << R$).

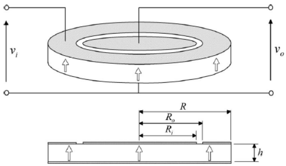

Figure: Construction of disk-PT

- The PT is polled in the thickness direction, and the two opposite surfaces are covered with electrodes
- The input and output electrodes are concentrically placed in top surface and the bottom surface is completely grounded.
- The input electrode is the external ring and output electrode is the inner ring.

Equivalent circuit model

- Research in the past[7] have made attempts to develop the equivalent electromechanical model of the piezoelectric transformer.

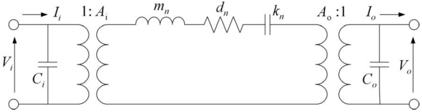

Figure: Equivalent electromechanical model of piezo-transformers

where $A_0 : A_1$ is the turns ratio, C_i and C_o are input and output capacitance, m_n is lumped mass, d_n is mechanical damping coefficient and k_n is the effective spring constant.

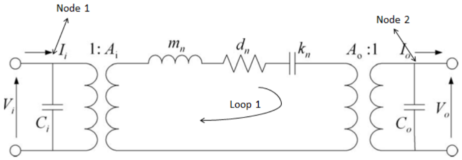

Applying KCL at nodes 1 and 2, KVL on loop 1, we end up with the following three fundamental equations.

$$(m_i s^2 + d_i s + k_i)X + A_o V_o = A_i V_i$$
$$sA_i X + sC_i V_i = I_i$$
$$sA_o X = sC_o V_o + I_o$$

Once the parameters in these equations are known, using these equations all other quantities of interest like efficiency, maximum power-transfer condition, effect of loading etc. can be determined.

Outline

Numerical simulation

- Disk based resonators which use the radial mode of vibration for disks with a ring-dot structure were simulated.
- The inner electrode is patterned as a disk (dot) and is the output and the outer annular electrode is lithographically separated by it (150 um) to form the input electrode (ring) forming the required ring-dot structure.
- This simulation was done for a 1 mm radius disk.
- The devices made were 1.5 mm so had a lower operating frequency.

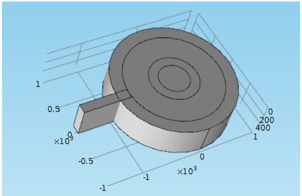

Simulation results

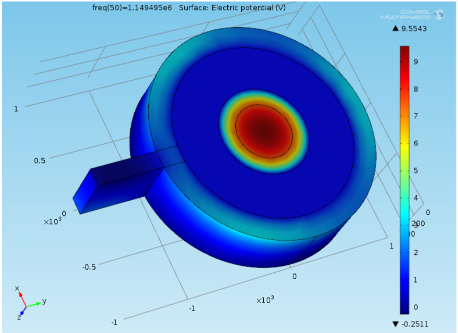

Figure: Surface potential profile of the disk resonator

Simulation results

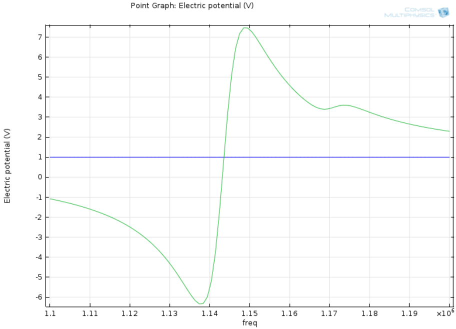

Figure: Output voltage (for 1V input) vs input frequency

Simulation results

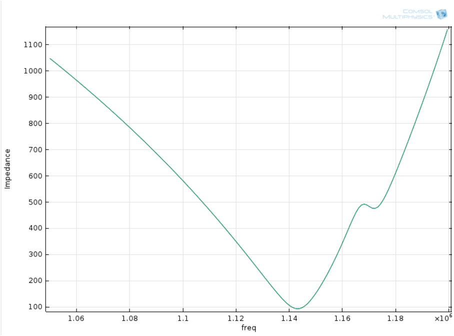

Figure: Impedance vs input frequency

- Both simulation and experiment indicated a very small input impedance at resonance ($70 - 100\Omega$)
- Hence, to prevent loading effects in the function generator, a unit-gain buffer is added before the input stage.

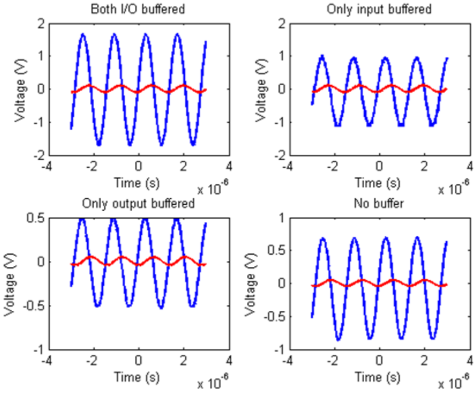

Figure: Input waveform (in red) and Output waveform (in blue)

- We were able to produce a maximum gain of 16 and also at a micro-scale which is a way better than other research work in this area.

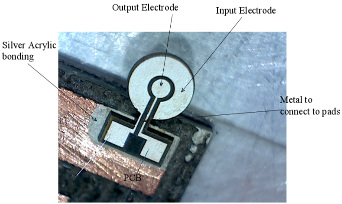

Figure: Image of the fabricated-disk transformer

Construction and working principle

- The source comprises a z-cut lithium niobate with an attached resistive heater on the top.
- The heater is placed on $+$z plate of the crystal and -z plate of the crystal is exposed to the ambient air.
- The heater is composed of a 68 Ω, 0.5-W resistor, which was epoxied to the crystal with a commercial thermal adhesive.
- DC current is passed through the resistor heating it up and therefore increasing the $+$z surface temperature of the crystal
- The change in potential V on the face of the crystal in response to a change in temperature ΔT is given by

$$V = d_{cr}\Phi\Delta T/\epsilon_{cr}$$

where d_{cr} is distance between the two plates, Φ is pyro-coefficient and ϵ_{cr} is the dielectric constant.

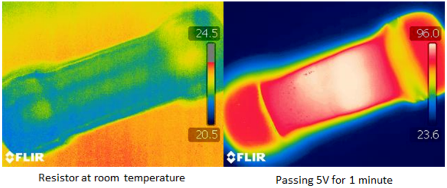

Figure: Temperature profile of the resistive heater on the top

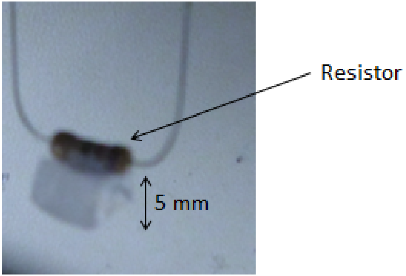

Testing and result

- Lithium Niobate ($LiNb0_3$) has $\Phi = 70\mu C/(m^2 K)$ and $\epsilon_{cr} = 30\epsilon_0$.
- The device has $d_{cr} = 5mm$ and change in temperature after 1 min ($\Delta T \approx 70K$).
- Using the equation $V = d_{cr}\Phi\Delta T/\epsilon_{cr}$, we calculate potential developed to be$V = 9.22\text{x}10^4\text{V}$ if no discharging occurred.
- But in ambient air, electric discharge happens much before.
- Electric ionization of ambient air occurred which could be heard as cracking sound in a silent room.

Some more designs-Quick overview

Here are few designs which are simulated but yet to be tested.

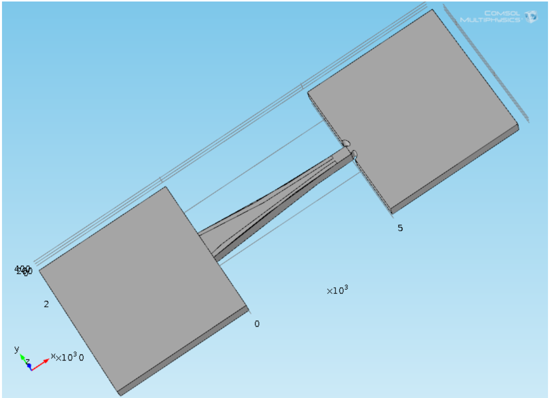

Figure: A beam supported at both the sides. Catenary horn is to amplify the displacement at the end where it is present and cuts act as stress amplifiers

Some more designs-Quick overview

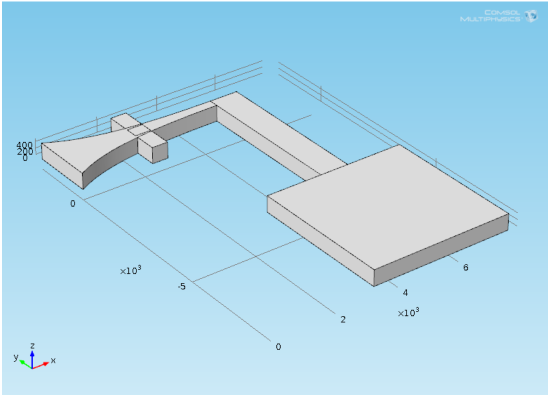

Figure: Ultrasonic horn actuator driving the cantilever beam

Some more designs-Quick overview

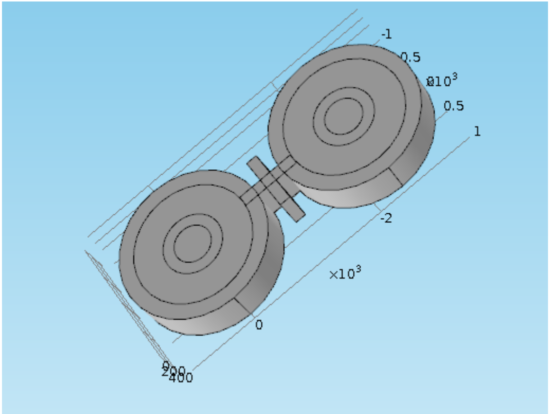

Figure: Two stage-cascaded disc resonators

Summary

- Producing HV from cantilever beam seems to be a new and novel idea.

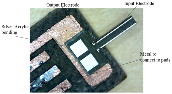

Figure: Micro-machined cantilever beam

- There is a need to improve the quality factor and the amplitude of oscillations.
- One way to go ahead will be to use the ultrasonic horn actuator to drive the cantilever beam.
- The output sense electrode capacitance should be minimized to produce more voltage for a given charge.
- Work also needs to be done on ensuring that the charges produced don't leak-through to the ground.

References I

[1] Ved Gund, Serhan Ardanuc, Yue Shi and Amit Lal
Low-voltage (<5V) ion-mobility spectrometer array for label-free gas detection
IEEE Transducers, pp. 2767-2770, 2013

[2] H.Revercomb & E.Mason
Theory of plasma chromatography/gaseous electrophoresis a review
Analytical Chemistry, vol. 47, pp. 970-983, 1975

[3] Sachin Nadig, Serhan Ardanuc and Amit Lal
Planar Laser-Micro Machined Bulk PZT Bimorph For In-Plane Actuation
UFFC 2013

References II

[4] C.A Rosen
Ceramic transformers and filters
Proceedings of electronic comp. symp., pp.205-211, 1956

[5] S.-T. H. S.-T. Ho
Modeling of a disk-type piezoelectric transformer
IEEE Trans. Ultrason. Ferroelectr. Freq. Control, vol. 54, pp. 21102119, 2007

[6] K.-T. Chang and C.-W. Lee
Fabrication and characteristics of thin disc piezoelectric transformers based on piezoelectric buzzers with gap circles
Ultrasonics, vol. 48, pp. 9197, 2008

THANK YOU